Structure, Vol. 10, 1669–1676, December, 2002, ©2002 Elsevier Science Ltd. All rights reserved. PII S0969-2126(02)00906-1

Large Conformational Changes in the Catalytic Cycle of Glutathione Synthase

Arhonda Gogos[1] and Lawrence Shapiro[1,2,3,4]
[1]Department of Biochemistry and Molecular Biophysics
[2]Department of Ophthalmology
[3]Naomi Berrie Diabetes Center
Columbia University College of Physicians and Surgeons
630 West 168th Street
New York, New York 10032

Summary

Glutathione synthase catalyzes the final ATP-dependent step in glutathione biosynthesis, the formation of glutathione from γ-glutamylcysteine and glycine. We have determined structures of yeast glutathione synthase in two forms: unbound (2.3 Å resolution) and bound to its substrate γ-glutamylcysteine, the ATP analog AMP-PNP, and two magnesium ions (1.8 Å resolution). These structures reveal that upon substrate binding, large domain motions convert the enzyme from an open unliganded form to a closed conformation in which protein domains completely surround the substrate in the active site.

Introduction

Glutathione functions in maintaining the reducing chemical environment in living cells, which is important for many biological processes. These include protection of cells against reactive oxygen species (ROS), maintenance of protein thiols in the reduced state, and maintenance of reduced ascorbic acid [1–3]. Glutathione also functions as a redox partner in the formation of deoxyribonucleotides from ribonucleotides, and as a cofactor for several enzymes [1, 3]. A progressive depletion in glutathione content in humans has been associated with human immunodeficiency virus (HIV) [4] and hepatitis C infections, as well as type II diabetes, adult respiratory distress syndrome, and other diseases. Low glutathione level is also a primary risk factor for the development of cataracts [3].

Glutathione is synthesized in two ATP-dependent steps. First, γ-glutamylcysteine (GGC) synthase catalyzes the formation of GGC. The final step is catalyzed by glutathione synthase:

$$\gamma\text{-glutamylcysteine} + \text{glycine} + \text{ATP} \rightarrow$$

$$\text{glutathione} + \text{ADP} + P_i$$

The ligation reaction is thought to proceed in the following manner [5–7]: The C-terminal carboxylate of GGC is phosphorylated by transfer of the γ-phosphate group of ATP to form an acylphosphate intermediate. Nucleophilic attack on this intermediate by glycine leads to the formation of a tetrahedral carbon intermediate, which dissociates to form the products glutathione, inorganic phosphate, and ADP.

Two forms of glutathione synthase deficiency in humans have been described: a mild form, referred to as glutathione synthase deficiency of erythrocytes, which causes hemolytic anemia, and a more severe form that causes 5-oxoprolinuria. This severe form is characterized by massive urinary excretion of 5-oxoproline, metabolic acidosis, hemolytic anemia, and central nervous system damage [8–11].

Glutathione synthase (GS) functions as a homodimer [12], and belongs to the ATP-grasp enzyme superfamily. The members of this family exhibit carboxylate-amine/thiol ligase activity and have a wide range of substrates [13, 14]. The structure of human glutathione synthase in complex with glutathione, ADP, and two magnesium ions was previously determined [7], however, the structure of the free enzyme is unclear. Here we describe the structure of yeast glutathione synthase in both the unbound form and in complex with its substrate γ-glutamylcysteine and the nonhydrolizable ATP-analog AMP-PNP. Comparison of these structures reveals substantial conformational changes in which the free enzyme, which adopts an open conformation, grasps the substrate and ATP-analog by forming new secondary structure elements and bringing two domains, which are distant in the free structure, into close apposition to form an enclosure around the ligands.

Results and Discussion

The structures reported here were determined in the following way. First, the structure of the apo form of the yeast GS was determined to 2.3 Å resolution by molecular replacement using the human product-complex structure as search model [15]. This structure was refined and then used as the search model for determination of the substrate-complex structure, which was ultimately refined to 1.8 Å resolution (Table 1, Figure 1). The free and substrate-bound enzymes crystallize in two unrelated lattices, each of which contained two molecules per asymmetric unit, corresponding to the physiological dimer.

Structure of the Ligand-Bound Enzyme

Overall Structure

The structure of yeast GS in complex with both GGC and AMP-PNP/Mg^{2+} (Figure 2A) is similar to that of the human enzyme (sequence identity 35%) in complex with the reaction products ADP and glutathione [7]. For the sake of clarity, we have retained the secondary structure nomenclature used for the human enzyme, and have denoted elements unique to the structure presented here with primes (Figure 3).

There are two crystallographically independent mole-

[4]Correspondence: shapiro@convex.hhmi.columbia.edu

Key words: Glutathione synthase; ATP-grasp superfamily; substrate complex; product complex; crystal structure; conformational change

Table 1. Statistics from the Crystallographic Analysis

Diffraction Data Statistics		
Crystal	GS	GS + ligands
Wavelength (Å)	0.9794	1.040
Resolution (Å)	20–2.3	20–1.8
Measured reflections	57,3251	505,425
Unique reflections	45,753	91,335
Completeness[1]	98.5% (100.0%)	97.2% (95.4%)
R_{sym}[2]	0.125 (0.177)	0.066 (0.40)
$\langle I \rangle / \langle \sigma I \rangle$	9.8	15.17
Refinement Statistics		
	GS	GS + ligands
Resolution range	20–2.3	20–1.8
Number of reflections (observed)	44,565	88,565
Number of reflections (R_{free})	2340	4433
R factor/R_{free}	0.216/0.237	0.172/0.196
Rmsd bond lengths	0.010	0.011
Rmsd bond angles	1.3	1.6
Rmsd dihedral angles	23.5	23.2
Rmsd improper angles	0.86	0.97

$R_{sym} = I - \Sigma|I - \langle I \rangle|/\Sigma I$, where I is observed intensity and $\langle I \rangle$ is average intensity. $R_{cryst} = 100 \times \Sigma||F_{obs}| - |F_{calc}||/\Sigma|F_{obs}|$ where F_{obs} are the observed structure factors and F_{calc} are the calculated structure factors. The crystallographic R factor, R_{cryst}, is based on 95% of the data used in refinement, and the free R factor, R_{free}, is based on 5% of the data withheld for the crossvalidation test. Rmsd, root mean square deviation. Over 90% of the main chain dihedrals fall within the "most favored regions" of the Ramachandran plot [22].

[1] Completeness for the highest resolution shell in parenthesis.

[2] R_{sym} for the highest resolution shell in parenthesis.

cules per asymmetric unit. The current model includes residues 6–491 of molecule 1, with no electron density apparent for residues 211–215; for molecule 2, residues 5–491 have been modeled, with regions 211–216 and 387–388 lacking clear electron density. In addition, each monomer is bound with one GGC molecule, one AMP-PNP, and two magnesium ions at the active site.

The overall structure is composed of two domains, a large "main" domain and a smaller "lid" domain. The main domain is characterized by an α/β-fold comprised of two topological subdomains: one of these is formed by a set of helices packed against an antiparallel β-sheet, and the other by a set of helices that pack against a parallel β-sheet. These two subdomains pack together to form the single globular main domain.

The smaller "lid" domain, which includes residues 355–417, consists of an antiparallel β sheet with helices packed on one side, and is situated as a protrusion that

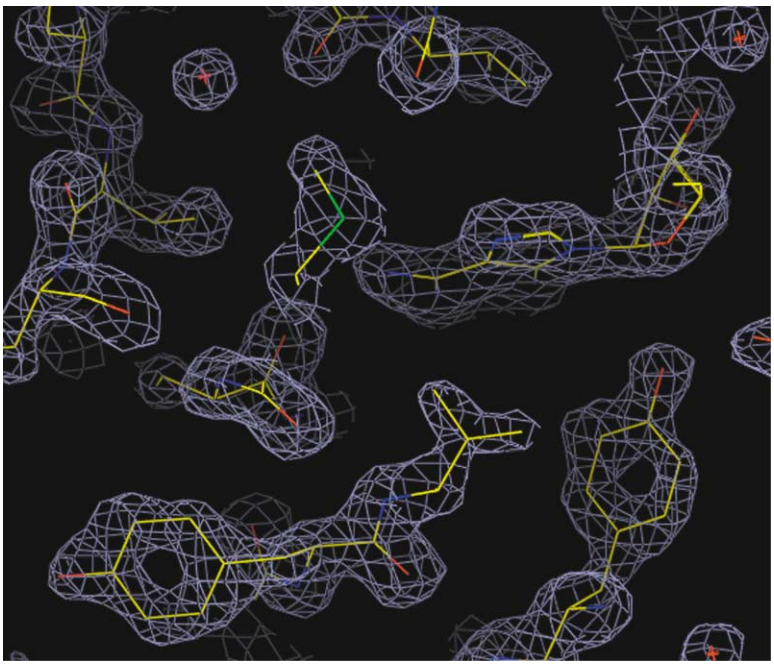

Figure 1. Electron Density Maps

Sample region of the $3f_{obs}$-$2f_{calc}$ electron density map for the liganded form of yeast GS, contoured at 1.5σ, showing part of the active site with the final refined model.

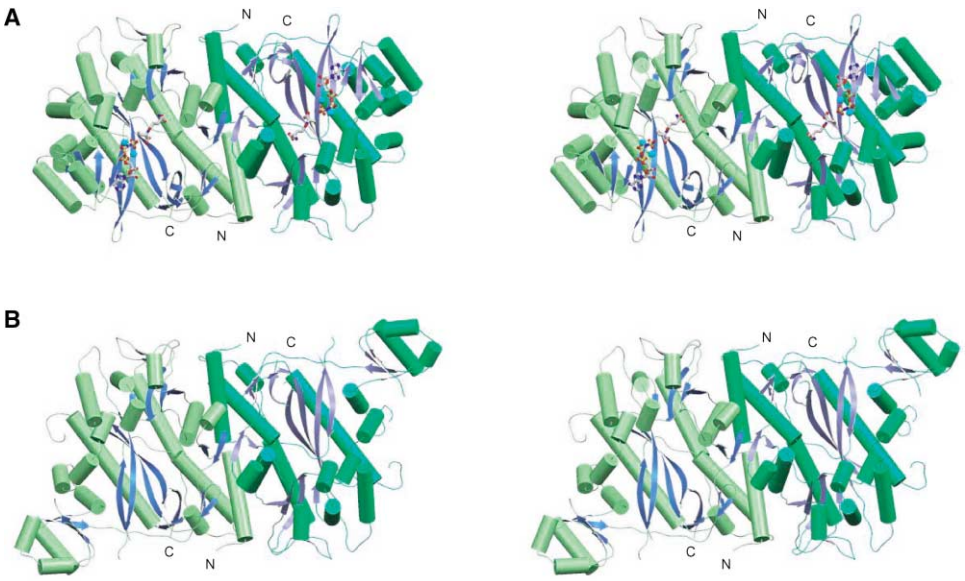

Figure 2. Overall Structure

Ribbon diagrams of (A) the yeast glutathione synthase dimer bound to γ-glutamylcysteine, AMP-PNP, and 2 magnesium ions per monomer, and (B) the yeast glutathione synthase dimer. Helices are shown as cylinders, and the NH_2- and COOH-termini are indicated. γ-glutamylcysteine and AMP-PNP are shown in an all-atom representation and the magnesium ions are shown as cyan spheres.

topologically connects the two subdomains of the main domain. The active site, which is clearly demarcated by the bound ligands, is formed at this interface by residues contributed by both the lid and main domains. A β sheet and a glycine-rich loop from the lid domain form part of the Mg^{2+}/ATP binding site and make extensive contacts

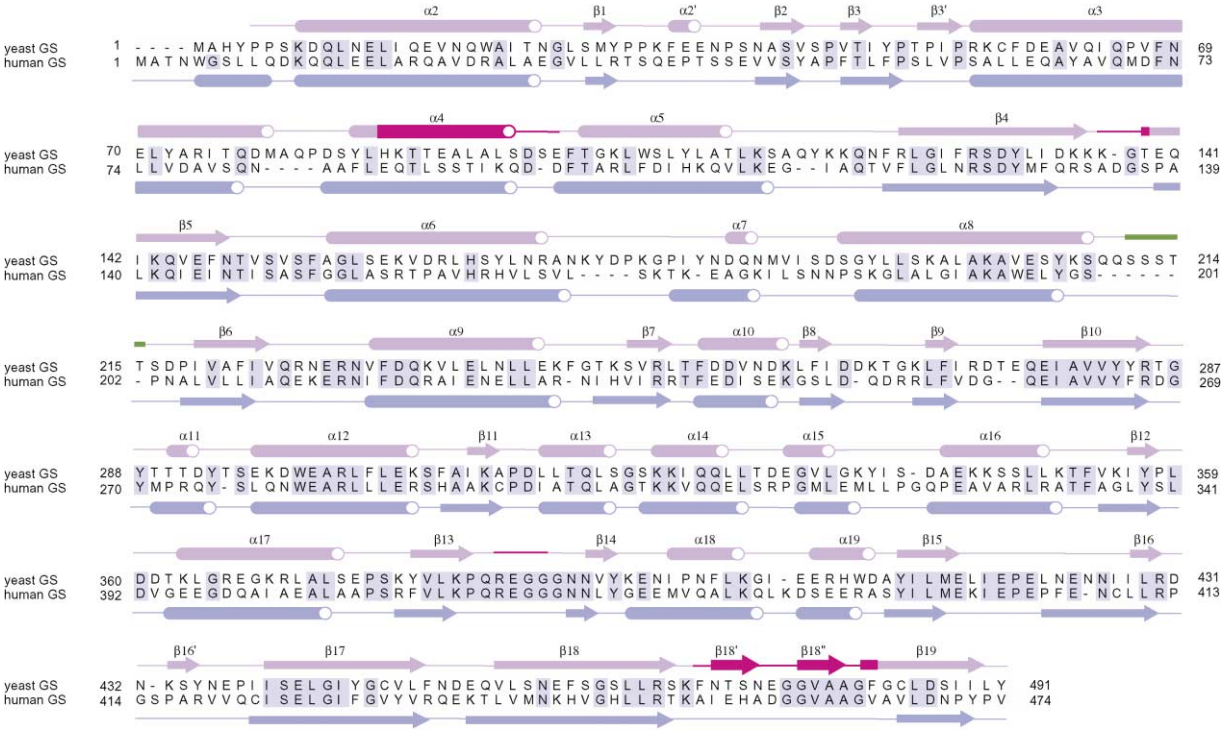

Figure 3. Structure-Based Sequence Alignment of Yeast Glutathione Synthase and Human Glutathione Synthetase

The corresponding secondary structure elements are shown above (yeast) and below (human) the alignment. Secondary structure differences are denoted with primes. The elements shown in red are disordered in the unliganded form of yeast glutathione synthase. The loop shown in green is disordered in the ligand-bound enzyme. Sequence identities are highlighted in purple.

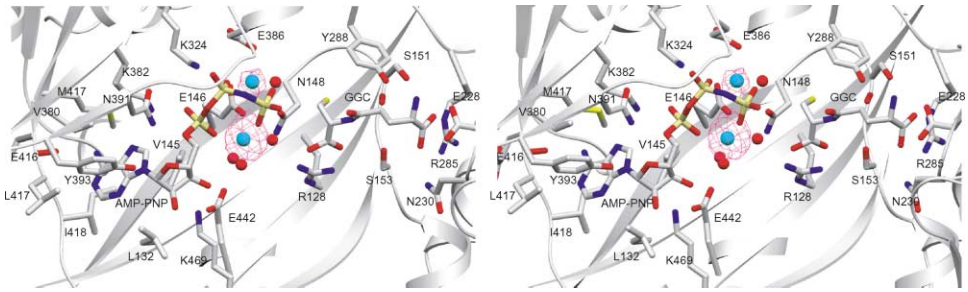

Figure 4. Binding of γ-Glutamylcysteine (GGC), AMP-PNP, and 2 Magnesium Ions to the Active Site of Glutathione Synthase

The ligands are shown in an all-atom representation, with the magnesium ions as cyan spheres and the water molecules as red spheres. Residues Leu132, Val145, Val380, Met415, Leu417, and Ile418 form a hydrophobic adenine binding pocket. There are hydrogen bonding interactions between adenine N6 and carbonyl oxygen of Glu416, ribose O2′ with Nζ of Lys469, O3′ with Oϵ2 of Glu442, O4′ with the hydroxyl group of Tyr393, and O5′ with to Nδ2 of Asn391. The side chains of lysines 324 and 382 form salt bridges with the α and β phosphates.

Magnesium 1 is coordinated by oxygen atoms from α and γ phosphates, Oϵ1 of Glu146, and 3 water molecules. Magnesium 2 is coordinated by oxygen atoms from the β and γ phosphates, Oϵ1 of glu386, both side chain oxygen atoms of Glu146, and a water molecule, which is coordinated by Asn148 Oδ1. The carboxylate oxygens of the γ-glutamyl moiety of GGC form a salt bridge with Arg285 and are within hydrogen-bonding distance from Ser153 and Asn230. The amide nitrogen is in hydrogen-bonding distance from Oϵ2 of Glu228, OH2 of Tyr288, and the carbonyl oxygen of Arg285. The carboxylate oxygens of the cysteine moiety form a salt bridge with Arg128 and are in hydrogen-bonding distance from the amide of Ser153. The amide of the cysteinyl moiety hydrogen bonds to the carbonyl oxygen of Ser151 and to Oγ of Ser153. There are 2 conformations for AMP-PNP and GGC present in our structure. These conformations affect the positions of the phosphates and the position of the thiol group, respectively. For clarity, we show only one conformation for each ligand in this figure.

Gd^{3+} anomalous difference Fourier map, contoured at 9σ, is shown in magenta. Bivjoet mates were collected using the inverse beam geometry at beamline X4A of the National Synchrotron Light Source (R_{symm} = 5.4%, completeness = 92.1% to 2.5 Å resolution; λ = 1.5498 Å, $f_{Gd}'' \approx 13.3\ e^-$).

with the nucleotide ligand, thereby giving the appearance of a hinged lid.

A dimer interface, similar to that observed for the human structure, is formed between the two molecules of the asymmetric unit, thus forming a pseudo-2-fold axis. This dimer interface is formed mainly by contacts between the β2 strands, hydrophobic interactions between helix α2 from one monomer and helix α9 from the other, a salt bridge between Arg170 and Glu243, and additional van der Waals and hydrogen bonding contacts. The structures of the two monomers of the asymmetric unit are essentially identical, although symmetry constraints were not included in the refinement.

ATP and Mg Binding

ANP-PNP binds between strand pairs β4, β5 of the main domain and β13, β14 of the lid domain (Figure 4), with interactions similar to the binding of ADP in the human structure and other ATP-grasp proteins [7]. The hydrophobic adenine binding pocket includes Ile418, Leu132, Met415, Val380, Leu417, and Val145. Hydrogen bonds are found between adenine N6 and carbonyl oxygen of Glu416, and adenine N1 and the amide nitrogen of Ile418. Hydrogen bonding interactions of the ribose include ribose O4′ with the hydroxyl group of Tyr393, ribose O3′ with Oϵ2 of Glu442, and atom O2′ with Nζ of Lys469. Ribose O5′ hydrogen bonds to Nδ2 of Asn391, and the side chains of lysines 382 and 324 form salt bridges with the α and β phosphates. These interactions are highly conserved between the human and the yeast enzyme structures. In our structure, AMP-PNP has two different conformations that differ in the position of the phosphates. The γ-phosphate of one of these conformations is not visible. Notably, in the human product-complex structure, an ADP β-phosphate oxygen hydrogen bonds to the main chain amide of Gly370 (388 in yeast) of the glycine-rich loop. In our structure, this loop is moved back to accommodate the γ-phosphate of AMP-PNP.

The positions of two magnesium atoms have been confirmed by crystallization of the protein in the presence of Gd^{3+} as a magnesium analog, and acquisition of Bijvoet difference data. An anomalous difference Fourier map revealed peaks at the expected positions for the two magnesium ions (Figure 4).

Magnesium 1 is coordinated by an α-phosphate oxygen, an oxygen from γ-phosphate, Oϵ1 of Glu146, and 3 water molecules. This is similar to the Magnesium 1 coordination in the human structure, except in that structure, a sulfate oxygen takes the place of one of the water ligands which, notably, is coordinated by the carboxyl end of the GGC substrate in our structure.

Magnesium 2 is coordinated by oxygen atoms from the β-phosphate and the γ-phosphate, Oϵ1 of glu386, both side chain oxygen atoms of Glu146 and a water molecule. This water molecule is coordinated by Asn148 Oδ1. The corresponding residue in the human structure directly coordinates the magnesium ion. These differences from the human structure potentially reflect a structural transition between the substrate- and product-bound states of the enzyme.

Substrate Binding

The binding of γ-glutamylcysteine is very similar to the binding of glutathione in the human structure. There are extensive interactions of the γ-glutamyl and cysteinyl moieties with highly conserved residues that exhibit nearly identical binding modes in both structures. The γ-glutamyl moiety of GGC forms a salt bridge with functional groups from Arg285 and hydrogen bonds with Ser153, Asn230, and Glu228 (Arg267, Ser151, Asn216, and Glu214, respectively, in the human enzyme). The cysteine moiety forms a salt bridge with Arg128 and hydrogen bonds to Ser151 and Ser153 (see legend to

Figure 4 for details). Arg125, Ser149, and Ser151 are the corresponding residues in the human enzyme. The substrate has two conformations in our structure that differ in the position of the thiol group. Superposition of the human and yeast structures show that the sulfate ion bound in the human enzyme's active site is very close to the carboxyl end of the substrate in the yeast enzyme's active site. This sulfate is positioned in a way that suggests potential mimicry of the phosphate in the short-lived phosphoracyl reaction intermediate that is the ultimate glycine acceptor.

In the human product-complex structure, the glycine moiety of glutathione interacts through hydrogen bonds with the amides of Val461 and Ala462, which are in a loop referred as "the Ala-rich loop" [7]. This loop also interacts with residues of the lid domain, resulting in shielding of the active site from the solvent. The corresponding residues in the yeast structure (V478, A479) are part of β strands β18′ and β18″—two strands not observed in the product complex—which are positioned away from the active site. While the formation of these β strands may reflect differences in the reactant- and product-complexes, we note that these strands are also involved in a small crystal contact. However, this conformation leaves an open channel to the active site, which may provide the means of ingress for the final glycine reactant.

Structure of the Free Enzyme

The overall structure of the apo form of GS (Figure 2B) is similar to that of the complexed forms, except for (1) substantial alteration of the relative positions of the main and lid domains, and (2) the loss of secondary structure elements which are likely involved in stabilization of the active site. The current model comprises residues 5–491 for both monomers. Regions 87–99, 137–139, 385–388, and 470–482 of monomer 1 appear to be disordered, and residues 87–98, 137–139, 385–389, and 471–482 are apparently disordered in monomer 2. The structure of the two crystallographically independent monomers is essentially identical, although the mobility of the lid domain differs widely, as evidenced by B factor analysis. The dimerization interface is also very similar to that of the complex structure, giving no structural indication for cooperativity between the two active sites.

In the free enzyme structure, the lid domain rotates away from the main domain by 64°, leaving the active site residues completely exposed to solvent (Figure 5). The glycine-rich loop of yeast GS, which forms part of the Mg^{2+}/ATP binding site, is disordered in the apo enzyme. The free and liganded glutathione synthases (both yeast-substrate and human-product complexes) also differ in their secondary structure, with two strands and one helix observed in the liganded structures not seen in the free. These observations suggest that these complex-specific structural elements form upon ligand binding to the free enzyme.

Helix α4, spanning residues 87–97, appears to be disordered in the structure of the free enzyme, and is only observed in the liganded structures. Although there are no direct contacts between α4 and substrate molecules, the lid domain is positioned to come into close contact with residues of this helix when the enzyme is in the closed form. The side chain of Asp97, near the C-terminal end of helix α4, makes a salt bridge with the Nε atom of Arg385 in the glycine-rich loop of the liganded structures. We note that these are conserved residues, suggesting their function in snapping the lid closed. Crystal packing interactions involving the lid domain are negligible for the closed conformation, but could potentially contribute to stabilization of the open form of the enzyme.

The region from residue 470–482, which includes strands β18′ and β18″, is seen only in the liganded structures and, remarkably, in substantially different conformations in the substrate and product complexes. This region is apparently disordered in the free structure, although it should be noted that the data for the unliganded form is relatively weak, and this may partially contribute to the absence of electron density.

Likely Domain Movements in the Catalytic Cycle

Here we report structures of yeast glutathione synthase in the apo form and in complex with its substrate GGC and Mg^{2+}/AMP-PNP. This provides snapshots of two stages in the catalytic cycle of the enzyme. A third state, the complex with reaction products, is not yet known for the yeast enzyme; however, the previously determined structure of the closely related human enzyme may provide a good model for this state. Every secondary structure element proximal to the active site, including all those of the lid domain, the glycine-rich loop, and helix α4, which forms upon ligand binding, are conserved between the two enzymes. In the β18′–β18″ region, there are no insertions or deletions, and the sequence that includes the entire β18″ strand is completely conserved. This leads us to suggest that the conformational differences between the yeast prereaction complex and the human postreaction complex are likely to represent differences in the enzyme state rather than interspecies differences in structure.

A simplified view of the conformational changes likely associated with the catalytic cycle of glutathione synthase is presented in Figure 6. The free form of the enzyme exists primarily in an open conformation, poised to bind its ligands—GGC and Mg^{2+}/ATP. Binding of these ligands stabilizes the conformation in which the lid domain is closed, and is held in place by several interactions, including those with the newly formed helix α4. Although Mg^{2+}/ATP is held in place by the closed conformation of the lid domain, the active-site proximal region encompassing β18′–β18″ adopts a conformation that enables the retention of solvent accessibility to the active site, allowing for ingress of the final substrate, glycine. In the product complex, the β18′–β18″ region adopts a compact structure in which the active site is entirely occluded from solvent [7]. Further solvent shielding is achieved by the movement of the glycine loop, no longer restrained by the γ-phosphate of the ATP-analog, further into the active site. This product complex may partly mimic the phosphoracyl intermediate: a sulfate ion is positioned in the active site near the cysteine carbonyl in the likely position the phosphate group of a phosphoracyl intermediate would adopt.

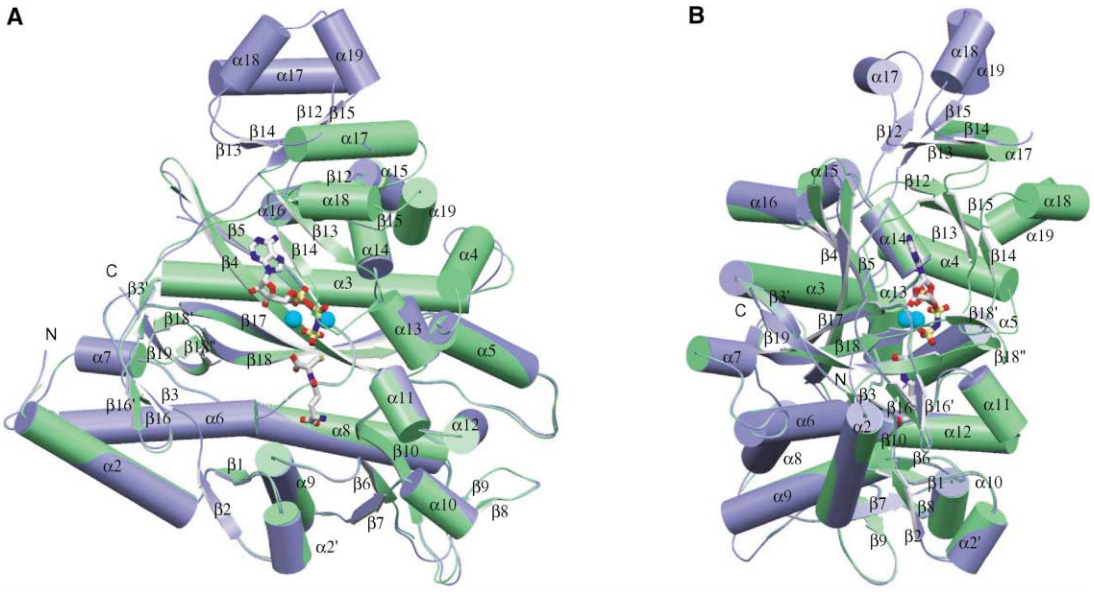

Figure 5. Movement of the Lid Domain Illustrated by Superposition of Main Domains in the Free and Liganded Forms

(A) The purple ribbon depicts a monomer of the unliganded form with the lid domain away from the active site and the enzyme in the open conformation. The green ribbon shows a monomer of the liganded form with the lid domain moving in to cap the active site, and the enzyme in the closed conformation Also note the formation of helix α4 in the closed form from residues that are disordered in the open form (residues 87–99).

(B) View 90° away from (A). Helices are shown as cylinders and the NH_2- and COOH-termini are indicated. γ-glutamylcysteine and AMP-PNP are shown in an all-atom representation and the magnesium ions are shown as cyan spheres.

Thus, this closed conformation may reflect the disposition of the enzyme during addition of the final glycine. Our results do not further understanding of the mechanism of product release.

Comparison to Other Members of the ATP-Grasp Superfamily

The structure of the human glutathione synthase revealed that, despite the lack of significant sequence identity, this enzyme shares core structural elements with the members of the ATP-grasp superfamily. Several prokaryote enzymes within this superfamily have yielded high-resolution structures, including the *E. coli* glutathione synthase (ecGS) and the *E. coli* biotin carboxylase [5, 7, 16, 17]. Although the spatial arrangement of domains is largely similar among the ATP-grasp proteins of known structure, the positions of some structural elements have been permuted in the linear sequences [7].

ecGS performs the same reaction as its eukaryotic counterparts, but has a different quaternary organiza-

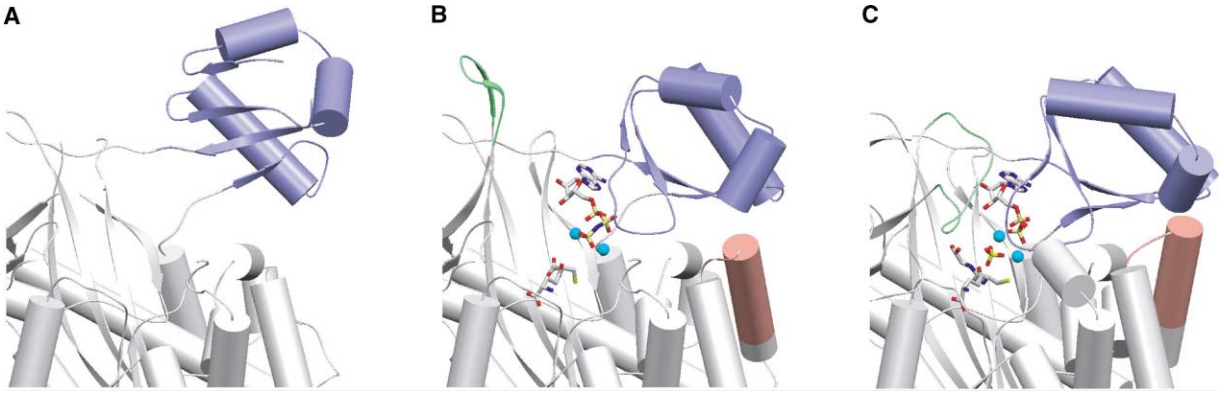

Figure 6. Snapshots of Conformational Changes in the Catalytic Activity of Glutathione Synthase

(A) Yeast glutathione synthase.

(B) Yeast glutathione synthase bound to its substrate γ-glutamylcysteine, AMP-PNP, and two magnesium ions.

(C) Human glutathione synthetase bound to the product glutathione, ADP, and two magnesium ions [7]. The lid domain is shown in purple, helix α4 is shown in orange, and the loop that includes strands β18′ and β18″ is shown in green. γ-glutamylcysteine, AMP-PNP, glutathione, and ADP are shown in an all-atom representation and the magnesium ions are shown as cyan spheres. See text for details.

tion, forming a tetramer in solution [17]. A detailed comparison of the product complexes of the *E. coli* and human enzymes demonstrated similar modes of ligand binding [7]. The two loops that cover the active site in the human structure are also present in the *E. coli* product complex [5]. These loops are invisible (disordered or flexible) in the free *E. coli* enzyme structure [17]. Nevertheless, helix α4 has no counterpart in the *E. coli* enzyme, and the lid domain is involved in dimer interactions and does not appear to undergo a large reorientation upon ligand binding.

E. coli biotin carboxylase is also dimeric, but the dimer interface is distinct from that reported here [7, 16]. Structures of the free biotin carboxylase enzyme and the enzyme bound to ATP revealed a 45° rotation of the lid domain upon nucleotide binding [16, 18], as compared to a 64° rotation for the structures reported here.

Biological Implications

Structures of yeast glutathione synthase in the presence and absence of substrate reveal large motions that convert the enzyme from an open to a closed conformation. A "lid" domain moves upon substrate binding to cap the ATP binding site and bring active site functional groups to their catalytic positions. A similar change in the disposition of the small and large domains of *E. coli* biotin carboxylase [18], also an ATP-grasp superfamily member, has been observed upon ATP binding. This suggests the possibility that open and closed conformations modulated by the presence or absence of nucleotide cofactor may be a functional mode common among ATP-grasp superfamily enzymes.

A glycine-rich loop of yeast GS, part of the lid domain, becomes ordered upon substrate binding, and forms part of the substrate binding pocket. An active site-proximal loop of the highly related human product-complex structure, which interacts with the glycyl moiety of glutathione, forms a β sheet in the yeast prereaction complex in the absence of glycine, leaving an open channel to the active site. The binding pocket around the substrate is very tight, except for this open channel, which could facilitate glycine access to the active site. Glutathione synthase achieves both accessibility of the active site to substrates and cofactors, and protection from solvent during catalysis through these dynamic structural rearrangements.

Experimental Procedures

Crystallization and Data Collection

Yeast glutathione synthase was expressed in *E. coli* as a 6His-tagged protein and purified to homogeneity by affinity chromatography, ion exchange chromatography on Q-sepharose, and gel filtration. The protein was concentrated to 17 mg/ml in 10 mM Tris-HCl (pH 8.0), 150 mM NaCl, and 1 mM DTT. Crystals of the unliganded enzyme were obtained by vapor diffusion in 2 μl hanging drops that contained equal volumes of protein and 1.97 M ammonium sulfate, 0.1 M Tris-HCl (pH 8.0), and 2% PEG 400 at 22°C. The space group was C2221 with a = 69.9 Å b = 155.1 Å c = 190.6 Å, with 2 protein molecules per asymmetric unit. Crystals of the liganded form were obtained after incubation with 3 mM γ-glutamylcysteine, 3 mM AMP-PNP, and 10 mM MgCl2 and using a well solution of 2.2 M ammonium sulfate, 0.1 M Tris-HCl (pH 8.0), 2% PEG 400, 5 mM TCEP, and 40 mM MgCl2 at 22°C. They belong to space group P1 with cell dimensions a = 51.7 Å b = 52.0 Å c = 100.6 Å α = 82.1° β = 86.8° γ = 77.5° and contain 2 protein molecules per asymmetric unit. The crystals were flash-frozen at 100°K in the well solution supplemented with 30% glycerol. Data was collected at beamline ID-32 of the Advanced Photon Source and at beamline X4A of the National Synchrotron Light Source (NSLS). The data was processed and merged with the HKL program suite [19]. The structure of the human glutathione synthase was used as a molecular replacement model for the apo form of yeast GS with the program Amore [15], which was subsequently used as a model for the substrate complex. Refinement was performed using CNS [20]. Figures were made using the program SETOR [21].

Acknowledgments

We gratefully acknowledge Kevin D'Amico at beamline ID-32 of the Advanced Photon Source and Craig Ogata at beamline X4A of the National Synchrotron Light Source (NSLS). We thank Titus Boggon for help with data collection and useful discussions, and Saurabh Patel for help with data collection. This is a contribution of the New York Structural Genomics Research Consortium (NIH S/G IP50 GM62529). Beamline X4A at the NSLS, a DOE facility, is supported by the Howard Hughes Medical Institute.

Received: July 2, 2002
Revised: September 25, 2002
Accepted: October 7, 2002

References

1. Meister, A., and Anderson, M.E. (1983). Glutathione. Ann. Rev. Biochem. *52*, 711–760.
2. Meister, A., and Larsson, A. (1995). Glutathione synthetase deficiency and other disorders of the glutamyl cycle. In The Metabolic Basis of Inherited Diseases, 7th Edition, C.R. Scriver, A.L. Beaudet, W.S. Sly, and Valle, D., eds. (New York, NY: Wiley), pp. 1461–1477.
3. Anderson, M.E. (1998). Glutathione: an overview of biosynthesis and modulation. Chem. Biol. Interact. *111–112*, 1–14.
4. Choi, J., Liu, R., Kundu, R., Sangiorgi, F., Wu, W., Maxson, R., and Forman, H. (2000). Molecular mechanism of decreased glutathione content in human immunodeficiency virus type 1 Tat-transgenic mice. J. Biol. Chem. *275*, 3693–3698.
5. Hara, T., Kato, H., Katsube, Y., and Oda, J. (1996). A pseudo-michaelis quaternary complex in the reverse reaction of a ligase: structure of Escherichia coli B glutathione synthetase complexed with ADP, glutathione, and sulfate at 2.0 A resolution. Biochemistry *35*, 11967–11974.
6. Artymiuk, P.J., Poirrette, A.R., Rice, D.W., and Willett, P. (1996). Biotin carboxylase comes into the fold. Nat. Struct. Biol. *3*, 128–132.
7. Polekhina, G., Board, P.G., Gali, R.R., Rossjohn, J., and Parker, M.W. (1999). Molecular basis of glutathione synthetase deficiency and a rare gene permutation event. EMBO J. *18*, 3204–3213.
8. Mohler, D.N., Majerus, P.W., Minnich, V., Hess, C.E., and Garrick, M.D. (1970). Glutathione synthetase deficiency as a cause of hereditary hemolytic disease. N. Engl. J. Med. *283*, 1253–1257.
9. Spielberg, S.P., Garrick, M.D., Corash, L.M., Butler, J.B., Tietze, F., Rogers, L., and Schulman, J.D. (1978). Biochemical heterogeneity in glutathione synthetase deficiency. J. Clin. Invest. *61*, 1417–1420.
10. Shi, Z.Z., Habib, G.M., Rhead, W.J., Gahl, W.A., He, X., Sazer, S., and Lieberman, M.W. (1996). Mutations in the glutathione synthetase gene cause 5-oxoprolinuria. Nat. Genet. *14*, 362–365.
11. Dahl, N., Pigg, M., Ristoff, E.G., Gali, R., Carlsson, B., Mannervik, B., Larsson, A., and Board, P.G. (1997). Missense mutations in the human glutathione synthetase gene result in severe metabolic acidosis, 5-oxoprolinuria, hemolytic anemia and neurological dysfunction. Hum. Molec. Genet. *6*, 1147–1152.
12. Whitbread, L., Gali, R.R., and Board, P.G. (1998). The structure

of the human glutathione synthetase gene. Chem Biol Interact. *24*, 35–40.
13. Murzin, A.G. (1996). Structural classification of proteins: new superfamilies. Curr. Opin. Struct. Biol. *6*, 386–394.
14. Galperin, M.Y., and Koonin, E.V. (1997). A diverse superfamily of enzymes with ATP-dependent carboxylate-amine/thiol ligase activity. Protein Sci. *6*, 2639–2643.
15. CCP4 (Collaborative Computational Project 4) (1994). The CCP4 suite: programs for protein crystallography. Acta Crystallogr. D *50*, 760–763.
16. Waldrop, G.L., Rayment, I., and Holden, H.M. (1994). Three-dimensional structure of the biotin carboxylase subunit of acetyl-CoA carboxylase. Biochemistry *33*, 10249–10256.
17. Yamaguchi, H., Kato, H., Hata, Y., Nishioka, T., Kimura, A., Oda, J., and Katsube, Y. (1993). Three-dimensional structure of the glutathione synthetase from Escherichia coli B at 2.0 A resolution. J. Mol. Biol. *229*, 1083–1100.
18. Thoden, J., Blanchard, C., Holden, H., and Waldrop, G. (2000). Movement of the biotin carboxylase B-domain as a result of ATP binding. J. Biol. Chem. *275*, 16183–16190.
19. Otwinowski, Z., and Minor, W. (1997). Processing of X-ray Diffraction Data Collected in Oscillation Mode. In Methods in Enzymology, Volume *276*, C.W. Carter and R.M. Sweet, eds. (London: Academic Press), pp. 307–326.
20. Brunger, A.T., Adams, P.D., Clore, G.M., DeLano, W.L., Gros, P., Grosse-Kunstleve, R.W., Jiang, J.S., Kuszewski, J., Nilges, M., Pannu, N.S., et al. (1998). Crystallography & NMR system: A new software suite for macromolecular structure determination. Acta Crystallogr. D Biol. Crystallogr. *54*, 905–921.
21. Evans, S.V. (1993). SETOR: hardware-lighted three-dimensional solid model representations of macromolecules. J. Mol. Graph. *11*, 127–138.
22. Laskowski, R.A., MacArthur, M.W., Moss, D.S., and Thornton, J.M. (1993). PROCHECK - A program to check the stereochemical quality of protein structures. J. Appl. Crystallogr. *26*, 283–291.

Accession Numbers

Coordinates have been deposited in the Protein Data Bank (accession codes 1M0T and 1M0W).